Science of the Total Environment 807 (2022) 150866

Contents lists available at ScienceDirect

Science of the Total Environment

journal homepage: www.elsevier.com/locate/scitotenv

When river water meets seawater: Insights into primary marine aerosol production

Jiyeon Park [a,*], Jiyi Jang [a,b], Young Jun Yoon [a], Sujin Kang [c], Hyojin Kang [a,d], Kihong Park [e], Kyung Hwa Cho [b], Jung-Hyun Kim [a], Manuel Dall'Osto [f], Bang Yong Lee [a]

[a] Korea Polar Research Institute, 26 Songdomirae-ro, Yeonsu-gu, Incheon 21990, South Korea
[b] School of Urban and Environmental Engineering, Ulsan National Institute of Science and Technology, UNIST-gil 50, Ulsan 44919, Republic of Korea
[c] Department of Marine Science and Convergent Technology, Hanyang University, 55, Hanyangdaehak-ro, Sangnok-gu, Ansan-si, Gyeonggi-do 15588, South Korea
[d] University of Science and Technology (UST), 217 Gajeong-ro, Yuseong-gu, Daejeon, Republic of Korea
[e] School of Earth Sciences and Environmental Engineering, Gwangju Institute of Science and Technology (GIST), 123 Cheomdangwagi-ro, Buk-gu, Gwangju 61005, South Korea
[f] Institut de Ciències del Mar, CSIC, Pg. Marítim de la Barceloneta 37-49, 08003 Barcelona, Catalonia, Spain

HIGHLIGHTS

- We conducted sea spray chamber experiments in Korean and Arctic coastal systems.
- The lowest number concentration of particles was observed in rive samples.
- Inorganic salts play a much larger role than organic matter in aerosol production.
- It should be considered when predicting its effect on climate under global warming.

GRAPHICAL ABSTRACT

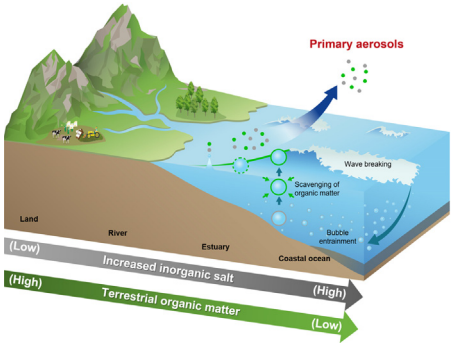

ARTICLE INFO

Article history:
Received 1 August 2021
Received in revised form 14 September 2021
Accepted 4 October 2021
Available online 7 October 2021

Editor: Pavlos Kassomenos

Keywords:
Primary marine aerosol
Chamber study
Inorganic salts
Organic matter
River-dominated coastal systems

ABSTRACT

The impact of inorganic salts and organic matter (OM) on the production of primary marine aerosols is still under debate. To constrain their impact, we investigated primary aerosols generated by a sea-spray generator chamber using surface water samples from rivers, estuaries, and seas that were collected along salinity gradients in two temperate Korean coastal systems and one Arctic coastal system. Salinity values showed an increasing trend along the river–estuary–coastal water transition, indicating the lowest amount of inorganic salts in the river but the highest amount in the sea. In river samples, the lowest number concentration of primary aerosol particles (1.01×10^3 cm^{-3}) was observed at the highest OM content, suggesting that low salinity controls aerosol production. Moreover, the number concentration of primary aerosols increased drastically in estuarine (1.13×10^4 cm^{-3}) and seawater (1.35×10^4 cm^{-3}) samples as the OM content decreased. Our results indicate that inorganic salts associated with increasing salinity play a much larger role than OM in aerosol production in river-dominated coastal systems. Laboratory studies using NaCl solution supported the conclusion that inorganic salt is a critical factor in modulating the particles produced from river water and seawater. Accordingly, this study highlights that inorganic salts are a critical factor in modulating the production of primary marine aerosols.

* Corresponding author.
E-mail address: jypark@kopri.re.kr (J. Park).

https://doi.org/10.1016/j.scitotenv.2021.150866

1. Introduction

Primary marine aerosol or sea spray aerosol (SSA) particles, produced through wave breaking on the ocean surface (Gong, 2003) are the largest source of natural aerosols to the atmosphere; therefore, they have a significant impact on Earth's radiation equilibrium (Partanen et al., 2014) and climate (Cochran et al., 2017). In addition to inorganic salts, SSA particles are heavily enriched in OM relative to their concentration in the surface ocean (Prather et al., 2013; Wang et al., 2017). For instance, the OM fraction in submicrometer SSAs increases up to 80% during oceanic phytoplankton blooms (Facchini et al., 2008). On a global scale, it is estimated that 8.0 ± 0.4 Tg yr^{-1} of primary submicrometer organic aerosols is emitted from the oceans to the atmosphere (Vignati et al., 2010; Spracklen et al., 2008). When OM is incorporated into global model simulations (Gantt et al., 2009; O'Dowd et al., 2008), satellite-derived chlorophyll *a* (Chl *a*) is used as a proxy for surface ocean biological activity in an effort to parameterize the emission of sea spray organics. This is based on findings from open oceans in the northeast Atlantic and the Southern Ocean, whereby Chl *a* was observed to be highly correlated with the OM fraction of ambient marine aerosols at both monthly and seasonal timescales (O'Dowd et al., 2004; O'Dowd et al., 2008; Sciare et al., 2009; Spracklen et al., 2008). In contrast, measurements of SSAs in the northwest Atlantic and the Californian Pacific Ocean have indicated that dissolved organic carbon (DOC) in surface seawater is the major source of OM to SSAs, regardless of the Chl *a* concentration (Bates et al., 2012; Quinn et al., 2014). Accordingly, it appears that oceanic Chl *a* concentrations may explain the variation in the OM fraction of SSAs downwind of plankton bloom regions in the open oceans. However, Chl *a* concentrations may not be applicable to other regions such as coastal oceans, where phytoplankton-derived Chl *a* accounts for only a small fraction of the OM in surface waters (less than 0.4% of OM) (Gardner et al., 2006; Huot et al., 2007; Quinn et al., 2015).

To date, aerosol production from wave breaking in freshwater systems such as lakes (known as lake spray aerosols), rivers, and estuaries has been far less studied in comparison to SSAs (Slade et al., 2010; May et al., 2016). As partially enclosed coastal waterbodies where river water and seawater mix, coastal estuarine systems are complex, productive coastal ecosystems connecting land and ocean (Ward et al., 2020; Canuel and Hardison, 2016). Estuaries are characterized by salinity gradients that range from rivers to oceans: 0.5‰ or less for river water, 0.5‰–29‰ for estuarine water, and approximately 35‰ for seawater. Previous studies have demonstrated the influence of salinity on the number size distribution of primary aerosol particles using NaCl solution or synthetic water (including only inorganic salts) (Russell and Singh, 2013; Mårtensson et al., 2003) but not for natural water samples (including both inorganic salts and OM) with different salinities. In terms of OM properties, unlike the open oceans, where phytoplankton production is the predominant source of OM (Whittle, 1977), the main sources of OM in estuaries can be divided into two categories: (1) terrestrial OM (allochthonous), which comes from soils and plant detritus (Yoon and Woo, 2013; Goni et al., 2008), and (2) in situ production (autochthonous) of phytoplankton, aquatic plants, and microbes (Martin et al., 2018; Small et al., 1990). Depending on the source and composition, estuarine OM exhibits a diverse reactivity (Galy et al., 2007) with a wide age range that extends back over 8000 ^{14}C years (Canuel and Hardison, 2016; Marwick et al., 2015). Therefore, variations in the concentration, source, composition, and age of OM along a river–estuary–coastal ocean salinity gradient play important roles in the regional carbon cycles of continental margins. However, the relative importance of such variations in the production of primary marine aerosol and atmospheric processes remains largely uncertain in coastal oceans. To date, only one study has been conducted in the river-influenced coastal oceans, demonstrating that terrestrial OM, mostly delivered from the Mackenzie River, can enhance primary aerosol production in the Arctic coastal region (Park et al., 2019). However, the authors did not consider the effect of OM characteristics (e.g., the molecular-level chemical composition and reactivity of OM) and on primary aerosol production under low salinity conditions (<19‰).

Here, we investigate the link between the complex source and age characteristics of OM in surface water samples, and primary aerosol production as a consequence of wave breaking along river–estuary–coastal ocean systems. Aerosol generation chamber experiments were performed using surface water samples (sampling water depth: 0 to ~50 cm) from a closed estuarine system (Geum) and an open (Seomjin) estuarine system in South Korea (Fig. 1). Primary aerosols were produced in a sea spray tank using three types of surface water samples taken along a salinity gradient: (a) river water (RW, i.e., freshwater), (b) estuarine water (EW, i.e., water from the interface of freshwater and saltwater mixing), and (c) seawater (SW, i.e., saltwater). The results from the two temperate Korean coastal systems were compared with the results of an Arctic chamber experiment (Park et al., 2019), which used water samples collected from the Mackenzie coastal system in September 2017 onboard the Korean icebreaker R/V *Araon* (Fig. 1). The objectives of this study are (1) to measure the number size distribution of primary aerosol particles; (2) to compare this with the concentration, chemical composition, source, and radiocarbon age of OM in the surface water samples; and (3) to assess how the quantity and chemical characteristics of inorganic salts and OM in the three types of water samples influence the properties of primary aerosols in the temperate and Arctic coastal systems studied here.

2. Materials and methods

2.1. Sample collection

Surface water samples were collected from the Geum and Seomjin coastal systems in May 2018 (Fig. 1 and Table S1). Surface water was collected directly into a high-density polyethylene carboy through Tygon tubing using an aspirator system. All samples were taken from the water surface at a depth of ~1 m. Both water salinity and pH were measured in situ using a Hydrolab DS5 multi-parameter water quality sonde (OTT Hydromet, Kempten, Germany). We obtained the total nitrogen (TN, mg L^{-1}), total phosphorus (TP, mg L^{-1}), and Chl *a* (mg L^{-1}) data from the Korean Water Environment Information System (http://water.nier.go.kr), and Water Resources Management Information System (http://www.wamis.go.kr). To investigate the effect of surface water OM on primary aerosol properties, we analyzed three surface RW samples from both rivers, four surface EW samples from the estuary transition zones, and four surface SW samples from the Yellow Sea and South Sea. The abbreviations GRW, GEW, and GSW represent RW, EW, and SW, respectively, sampled from the Geum estuary system. The abbreviations SRW, SEW, and SSW represent RW, EW, and SW, respectively, sampled from the Seomjin estuary system.

2.2. Bubble-bursting chamber experiments

Bubble-bursting experiments were conducted using a laboratory-scale sea spray tank of 5 L capacity filled with 3 L of each water sample (GRW, GEW, GSW, SRW, SEW, and SSW). Detailed information on the performance and operation of the tank has been previously described (Park et al., 2019). In brief, the water sample was pumped into the top of the tank at a constant rate of 3 L min^{-1} using an aquarium pump. Then, SSA particles were produced by splashing the water through plunging water jets, separated into eight jets, which could closely simulate the air entrainment caused by a breaking wave. During the experiments, the bubble flowrate and temperature inside the chamber system remained constant for all water samples. To ensure the absence of ambient room air, particle-free air was continuously supplied into the tank at a flow rate of 10 L min^{-1}. Before turning on the water jet, blank measurements were performed during the first 15 min of each experiment by verifying the total number concentration of particles in the

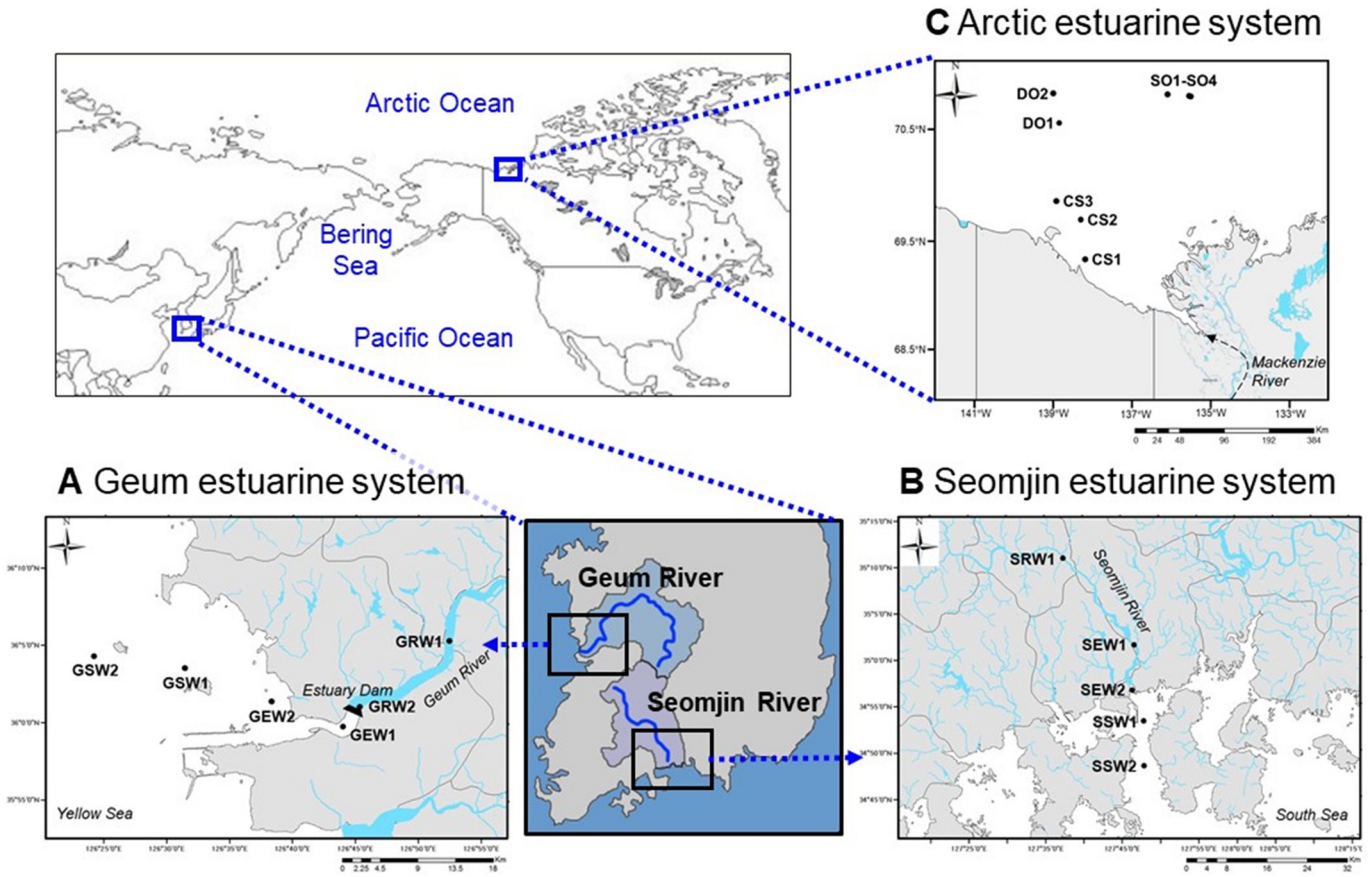

Fig. 1. Surface water sampling sites in the (A) Geum, (B) Seomjin, and (C) Arctic coastal systems.

air space of the tank. The value was zero, confirming that there was no leakage and no background particles. The SSA particles generated by this tank were dried using a series of diffusion dryers, and then the number size distribution of the dried SSA particles in the size range of 10 nm to 1 μm were measured. Before each experiment, the total number concentration of primary aerosol particles produced from deionized water was determined, which lasted approximately 2 h. The value was 53.43 cm^{-3}, ensuring that there was no secondary aerosol production (e.g., gas-to-particle conversion processes), contamination, or leakage inside the tank (Fig. 2). The sea spray tank was also used to produce primary aerosols using the RW, EW, and SW samples for comparison under consistent generation conditions.

2.3. Measurements of primary aerosol properties

The size distribution of primary aerosols in the size range of 7–300 nm was measured with a scanning mobility particle sizer (SMPS) (differential mobility analyzer (DMA), TSI 3081, USA; and condensation particle counter (CPC), TSI 3772, USA) every 3 min. In the SMPS system, the aerosol and sheath flow rates were 1.0 L min^{-1} and 10 L min^{-1}, respectively. An optical particle counter (OPC) (TSI 3330, USA) was also used to measure the size distribution of primary aerosols in the size range of 300 nm to 1 μm with a sample flow rate of 1.0 L min^{-1} every 3 min. The sizing calibration of SMPS (for DMA) and OPC was performed using a certified particle standard, such as polystyrene latex (PSL) particles of known sizes (152 nm PSL particles for SMPS and 2 μm PSL particles for OPC; Duke Scientific, USA), showing a good agreement within ~3%. To obtain the number size distribution of primary aerosol particles in the size range of 7 nm to 1 μm, we used SMPS data from 7 nm to 300 nm and OPC data from 300 nm to 1 μm. The OPC system was only used to generate the tail toward the primary aerosols larger than 300 nm, which was not detected by the SMPS system.

2.4. Characterization of OM in surface water samples

For the DOC and POC analyses, approximately 0.12 L of each water sample was filtered through pre-combusted (450 °C for 5 h), preweighed glass fiber filters (Macherey-Nagel, Duren, Germany; 0.45 μm pore size). Duplicates or triplicates were taken for each sample. After filtration, the filters were freeze-dried (−60 °C for 24 h) and then weighed to calculate the concentration of total suspended matter (TSM). Part of each filter (or the entire filter for POC analysis) was acidified with 12 M HCl to remove inorganic carbon for 24 h. The POC concentration, PN concentration, and $\delta^{13}C_{POC}$ were analyzed using an elemental analyzer combined with an isotope ratio mass spectrometer (Delta V, Thermo Fisher Scientific, Bremen, Germany or Isoprime visION, Elementar, Langenselbold, Germany). We used IAEA–CH–3 cellulose and IAEA–N–1 ammonium sulfate as working standards for determining the concentration and stable isotope ratio of POC and concentration of PN, respectively. The precision was <0.1% for POC concentration, <0.9% for PN concentration, and <0.1‰ for POC stable isotope ratio. All DOC and TDN samples were analyzed against surface seawater consensus reference material (CRM) supplied by the Hansell Laboratory University of Miami (Batch 17–2017, Lot#10-17 SSR, DOC: 70–73 μM, TDN: 3–5 μM). More than five CRM samples were analyzed on each analytical day, and precision was characterized by a relative standard deviation of <5% for both DOC and DTN. Radiocarbon analyses were conducted at the National Ocean Science Accelerator Mass Spectrometry Facility of the Woods Hole Oceanographic Institution (NOSAMS) in the USA and Alfred Wegener Institute (AWI) in Germany following standard protocols. The radiocarbon data of POC are presented in delta notation ($\Delta^{14}C_{POC}$, ‰).

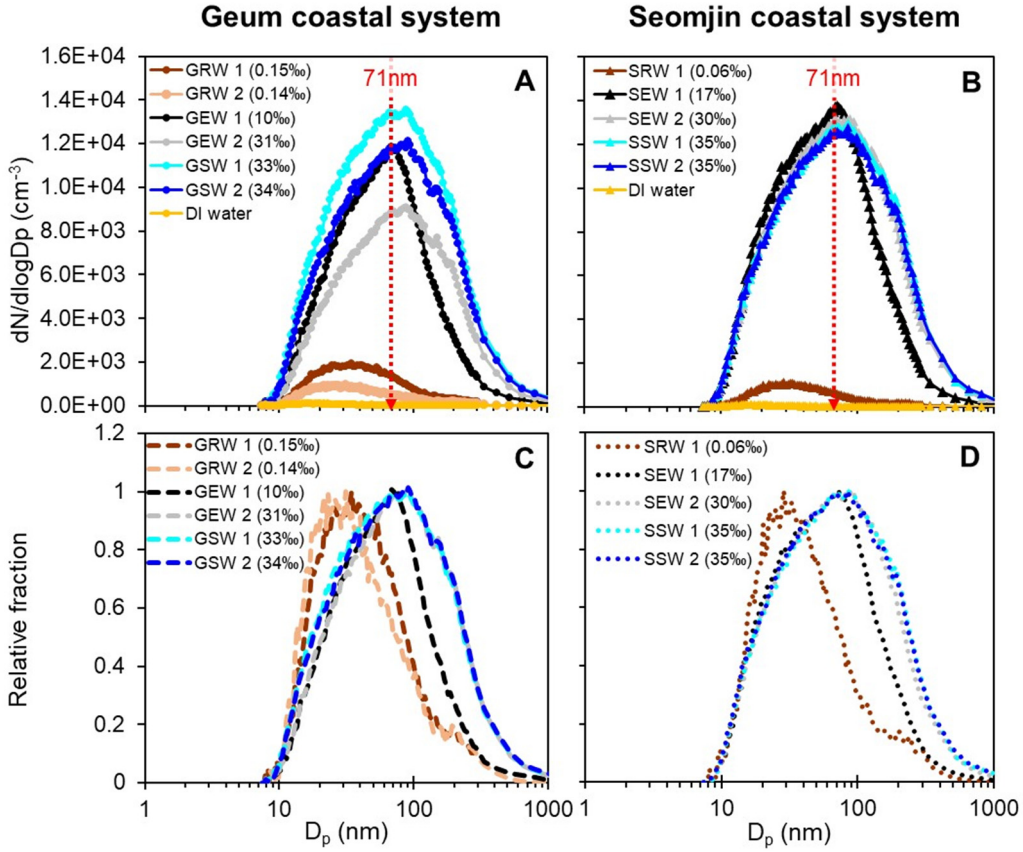

Fig. 2. Number size distributions of primary aerosol particles produced from surface water in the (A) Geum and (B) Seomjin coastal systems and relative fractions of primary aerosol particles produced from surface water samples from the (C) Geum and (D) Seomjin coastal systems. Values in parentheses indicate the water salinity.

A fraction of each filtered sample was immediately placed in a 40 mL amber vial with $HgCl_2$ to determine the DOC concentration and corresponding optical properties. The DOC and DTN concentrations of the filtered water samples were measured using a total organic carbon (TOC) analyzer (TOC-L; Shimadzu, Japan) equipped with a total nitrogen (TN) measuring unit (TNM-L; Shimadzu, Japan) and auto-samplers (ASI-L and ASI-V; Shimadzu, Japan) by the high-temperature combustion method. To determine the sources of DOC in the water samples, the optical properties and signatures of chromophoric and fluorescent DOC (i.e., CDOM and FDOM, respectively) were further analyzed. An ultraviolet-visible (UV-VIS) spectrometer (S-3100; Sinco, Korea) with 10 cm quartz cuvettes was used to measure CDOM. Deionized water was used as a reference, and the absorption spectra were scanned from 190 nm to 1100 nm at 1 nm intervals. The optical density at a specific wavelength of the measured absorbance was transformed into the CDOM absorption coefficient [$a_{CDOM}(\lambda)$] (m^{-1}). In this study, the CDOM value was derived at 375 nm, which is widely used as a proxy for terrestrial DOC. A subfraction of CDOM fluoresces is defined as the FDOM, which was measured by a Varian Cary Eclipse fluorescence spectrometer (Varian, USA). The excitation (EX)—emission (EM) matrices (EEMs) were collected using the EX spectra from 250 nm to 500 nm and the EM spectra from 280 nm to 600 nm. The EEM of deionized water was subtracted from the values of the analyzed samples to eliminate the water Raman signal. Based on the ranges of Coble (2007), it is possible to distinguish four different groups of fluorophores: terrestrial humic-like fluorescence (peaks A) (EX: 260 nm, EM: 380–460 nm), terrestrial fulvic-like fluorescence (peaks C) (EX: 350 nm, EM: 420–480 nm), marine humic-like fluorescence (peaks M) (EX: 310 nm, EM: 380–420 nm), and proteinaceous fluorescence (peaks T) (EX: 270 nm, EM: 340 nm).

To characterize the molecular DOM components, DOM was extracted as described by Hao et al. (2006) using solid-phase extraction (SPE) with a hydrophilic–lipophilic balanced (HLB) SPE cartridge (6 mL, 500 mg, Oasis-HLBTM, Waters, USA). The DOM extracts (10 μL) were injected into an Orbitrap Q-Exactive spectrometer (Thermo Fisher Scientific, Germany) coupled with liquid chromatography (Ultimate 3000, Dionex Co., USA). The Acclaim™ C18 column (2.1 mm × 150 mm, 2.2 μm, 120 Å, Thermo Fisher Scientific, USA) was used for chromatographic separation, with methanol as the mobile phase at a flow rate of 0.3 mL min^{-1} for 20 min. Mass spectra were acquired under a capillary temperature of 320 °C, and 3.8 kV (positive-ion) and 3.0 kV (negative-ion) of spray voltages in full scan mode (100–1500 *m/z*) at high resolution (140,000 FWHM). Mass spectra and formula assignment were conducted using a Thermo Xcalibur Qual Browser (ver. 2.5).

3. Results and discussion

3.1. Number size distribution of primary aerosol particles

We determined the number size distribution of primary aerosols in the size range from 7 nm to 1 μm for the surface waters sampled from the Geum and Seomjin coastal systems, as displayed in Fig. 2A and B. In the Geum coastal system, the salinity was extremely low in the upper parts of the dam due to the blockage of salinity diffusion (0‰ for the Geum RW (hereafter GRW) samples, see Supplementary Information Table S1). After the dam, the salinity drastically increased to 20 ± 14‰ for the Geum EW (hereafter GEW) samples as a result of freshwater–seawater mixing. The salinity of the Geum SW (hereafter GSW) samples was 33 ± 1‰, which is similar to that of typical regional seawater (i.e., approximately 32–33‰ for the Yellow Sea)

(Wei et al., 2010; Seo et al., 2017). Because salinity can be defined as the amount of inorganic salt (e.g., NaCl, KCl, $CaCl_2$, K_2SO_4, and $MgSO_4$) dissolved in water (Williams and Sherwood, 1994), such salinity changes revealed the lowest amount of inorganic salts in the GRW samples but the highest amount in the GSW samples. The total number concentration of primary aerosol particles generated from the GRW samples (1.12×10^3 cm^{-3}) was 8–12 times lower than that of primary aerosol particles generated from the GEW (9.39×10^3 cm^{-3}) and GSW (1.35×10^4 cm^{-3}) samples. As illustrated in Fig. 2C, the modal diameters of the aerosol particles for the GRW, GEW, and GSW samples were 32.9 ± 2.5 nm, 79.6 ± 12.2 nm, and 86.7 ± 2.2 nm, respectively.

In comparison to the Geum coastal system, the salinity along the Seomjin coastal system increased more gradually owing to the absence of a dam (Supplementary Information Table S1), with salinities of 0‰, 24 ± 10‰, and 35 ± 0.4‰ for the Seomjin RW, EW, and SW (hereafter SRW, SEW, and SSW) samples, respectively. The total number concentration of primary aerosol particles generated from the SRW samples with low salinity (8.02×10^2 cm^{-3}) was 17 times lower than those generated from the SEW (1.32×10^4 cm^{-3}) and SSW (1.36×10^4 cm^{-3}) samples with higher salinities. The modal diameters of primary aerosol particles generated from the SRW, SEW, and SSW samples were 23.9 ± 0 nm, 69.8 ± 1.8 nm, and 85.1 ± 0 nm, respectively (Fig. 2D).

For both coastal systems, the RW samples with a relatively low inorganic salt resulted in a very low production of primary aerosols that had a smaller size than other the EW and SW samples. This indicates that the number concentration and modal diameter of primary aerosol particles can be influenced by the amount of inorganic salts (associated with salinity level) in water samples. The production of smaller-sized primary aerosol particles in the RW samples may be related to the fact that the droplets produced by bubble bursting in freshwater had lower concentrations of inorganic salts (i.e., lower salinity and lower solute concentrations), thus forming smaller dry particles than those produced by bubble bursting in seawater (assuming the initial droplet was the same size) (Blenkinsopp and Chaplin, 2011; Slade et al., 2010). Relatively small-sized particles of ~46 ± 6 nm were also observed in freshwater samples from the Laurentian Great Lakes (May et al., 2016; Axson et al., 2016), and over Lake Michigan (Slade et al., 2010). Moreover, the modal diameters of primary aerosols generated from the GSW (86.7 ± 2.2 nm) and SSW (85.1 ± 0 nm) samples also agreed well with the modal diameters of primary SSAs created using laboratory generation techniques (May et al., 2016; Sellegri et al., 2006; Schwier et al., 2015).

Notably, the number size distributions of primary aerosols produced from the GEW 1 (salinity 10‰) and SEW 1 (salinity 17‰) samples with moderate salinity exhibited different features compared to the GSW (salinity 33‰) and SSW (salinity 35‰) samples with higher salinity (Fig. 2A–D). The modal diameter of the number size distribution for the GEW 1 and SEW 1 samples was approximately 71 nm. We note that, for the GEW 1 and SEW 1 samples, the number concentrations of primary aerosol particles of >71 nm were lower than those for the GSW and SSW samples due to the lower salinity; however, differences in the number concentration of primary aerosol particles of <71 nm between them were not significant. This suggests that the components of water samples other than salinity contributed to the enhancement of number concentration of smaller-sized primary aerosols (<71 nm) for the GSW 1 and SSW 1 samples. In general, aquatic systems are primarily composed of dissolved inorganic salts (e.g., Na^+ and Cl^-) and OM (e.g., particulate organic carbon (POC) and DOC). Thus, we inferred that the production of smaller-sized primary aerosol particles (<71 nm) from moderate salinity water was influenced not only by inorganic salts but also by the OM properties of the surface water samples. We discuss this in more detail in Section 3.3. For example, the chemical compositions and phase images of submicrometer film and jet drop particles were investigated using an intermittent plunging water sheet (Wang et al., 2017). The authors demonstrated that both particles had a core-shell structure that was typical of dry SSA particles: an inorganic salt core and an OM-rich shell.

3.2. OM properties in surface water

To elucidate the role of OM in the number size distributions of primary aerosols along a salinity gradient, we further characterized POC and DOC in the Geum and Seomjin water samples. The highest POC and particulate nitrogen (PN) concentrations were found in the RW samples for both coastal systems, and showed decreasing trends from the river sites to the sea sites (Fig. 3A and B). Typically, the $\delta^{13}C$ and $\Delta^{14}C$ characteristics of POC have been used to assess the source and age of OM (Raymond and Bauer, 2001). The lowest $\delta^{13}C_{POC}$ values were in the GRW (−29.41‰) and SRW (−25.09‰) samples, which gradually increased toward the GSW and SSW samples (Fig. 3C). Other studies have reported $\delta^{13}C_{POC}$ values of −28.0 ± 4.0‰ for terrestrial-derived POC (Marwick et al., 2015; Peterson and Fry, 1987; Meyers, 1997) and −20.0 ± 2.0‰ for marine-derived POC (Chen et al., 2008; Guo et al., 2015; Ye et al., 2017). Accordingly, the increasing trends of $\delta^{13}C_{POC}$ in the Geum and Seomjin coastal systems indicate that the contribution of terrestrial-derived OC to the total OC pool reduced seawards due to mixing with marine-derived OC. The trends of $\Delta^{14}C_{POC}$ in the two coastal systems were similar, with depleted values for the EW samples (Fig. 3D). Nonetheless, it is worth noting that the average $\Delta^{14}C_{POC}$ value of the GEW samples (−55.4 ± 60.8‰) was lower

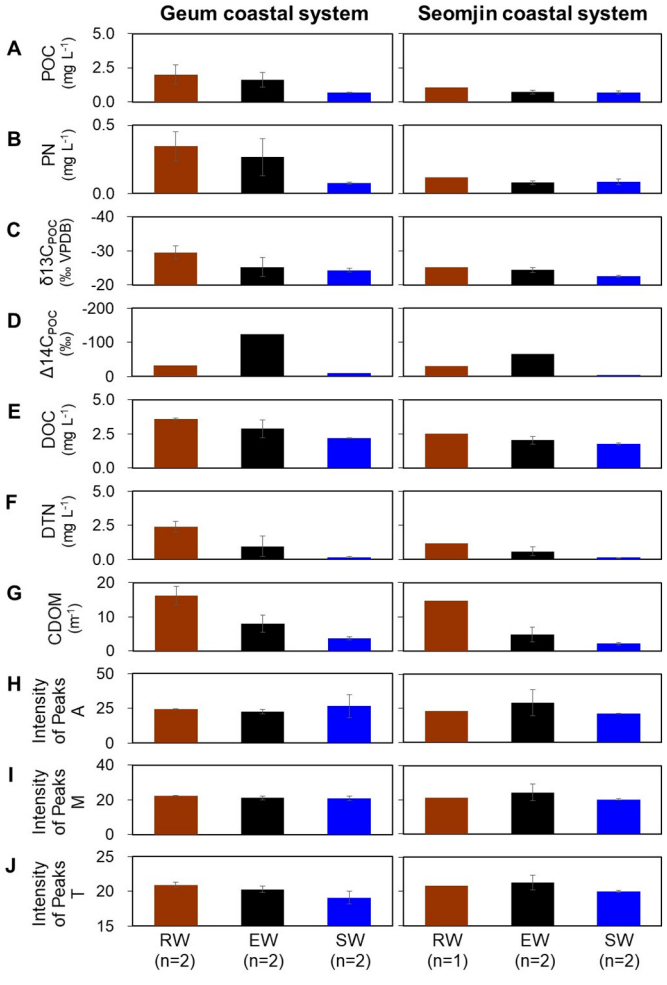

Fig. 3. Variations in (A) particulate organic carbon (POC), (B) particulate nitrogen (PN), (C) stable carbon isotopes of POC ($\delta^{13}C_{POC}$), (D) radiocarbon isotopes of POC ($\Delta^{14}C_{POC}$), (E) dissolved organic carbon (DOC), (F) dissolved total nitrogen (DTN), (G) chromophoric DOM (CDOM), and (H-J) fluorescence intensities in the Geum and Seomjin coastal systems. H, I, and J represent the fluorescence intensities of peak A (terrestrial humic-like substances), peak M (marine humic-like substances), and peak T (proteinaceous substances), respectively. The error bars represent the standard deviation according to the number of samples (n).

than that of the SEW samples (−33.3 ± 31.4‰). This suggests that the contribution of older POC to the total POC pool was larger for the GEW samples than for the SEW samples, which might be associated with the resuspension of reworked older bottom sediments due to tidal currents (Kang et al., 2020).

The DOC concentration also exhibited a decreasing trend from the RW to SW sampling sites, reducing from 3.64 mg L^{-1} to 2.19 mg L^{-1} in the Geum coastal system, and from 2.53 mg L^{-1} to 1.71 mg L^{-1} in the Seomjin coastal system (Fig. 3E). The dissolved total nitrogen (DTN) and DOC concentrations presented similar patterns (Fig. 3F). As the light-absorbing fraction of dissolved OM (DOM), chromophoric DOM (CDOM) has been commonly used as an optical proxy to evaluate the relative levels and spatial distributions of terrestrial-derived DOC in aquatic environments (Mannino et al., 2008; Li et al., 2017). The highest CDOM absorption values were in the GRW 2 (18.21 m^{-1}) and SRW 1 (14.72 m^{-1}) samples (Fig. 3G), indicating elevated inputs of terrestrial-derived DOC at these sites. A significant positive correlation was obtained between DOC concentrations and CDOM values for the Geum ($R = 0.93$) and Seomjin ($R = 0.96$) coastal systems (Fig. S1). These results suggest that the dominant source of DOC in both coastal systems was of terrestrial origin (e.g., plant- and soil-derived DOC). A previous study in the Geum and Seomjin systems found that a potential DOC source at the same sites might be a mixture of C_3-derived forest soils and cropland OM (Kang et al., 2019). As a subfraction of CDOM, fluorescent DOM (FDOM) allows us to distinguish between different groups of fluorophores, such as terrestrial humic-like substances (peaks A), marine humic-like substances (peaks M), and protein-like substances (peaks T) (Fig. S2). The differences in the three fluorescence intensities of peaks A, M, and T between the sample groups were minor (Fig. 3H–J), suggesting that the sources of the fluorescent components were similar. In addition, non-significant changes in protein-like substances (i.e., peaks T), which are usually characterized as amino acid-like DOM derived from the ocean, were observed for all samples, indicating little impact of marine-derived OM (e.g., phytoplankton and bacteria) on the properties of DOM.

High-resolution mass spectrometry can provide a large number of empirical formulae based on DOM samples, including those of lipid-like, protein-like, carbohydrate-like, unsaturated hydrocarbon-like, lignin-like, tannin-like, and condensed aromatic structures (CAS), as displayed in the van Krevelen diagrams (Fig. S3). The highest intensities of lignin-like substances (42%–64%) were observed for all water samples (Fig. S4). Furthermore, larger amounts of lignin-like substances were found in the GRW and SRW samples in comparison to the GSW and SSW samples. Lignin provides an important tracer for plant-derived products (also called terrestrial DOM), and various types of lignin are regarded as refractory compounds. Their contribution to DOM accumulates along riverine pathways as a result of slower remineralization; thus, lignin concentrations are relatively high in the oceans (Nebbioso and Piccolo, 2013). A previous study analyzed the molecular compositions of organic aerosols in the atmosphere over the Arctic during the spring–summer period using an ultrahigh-resolution mass spectrometer (Choi et al., 2019). The authors found that lignin compounds accounted for approximately 30% of the total assigned molecular formulae when the air masses mainly passed over the ocean region. These results indicate that the accumulation of OM potentially derived from terrestrial sources in the Arctic Ocean could influence the chemical characteristics of Arctic organic aerosols. Hence, the molecular mass data of DOM from the two Korean coastal systems hint at the potential direct emission of terrestrial lignin-like organic compounds from surface water into the atmosphere via bubble bursting processes.

3.3. Influence of inorganic salts and OM in water samples on primary aerosol properties

To investigate how inorganic salts and OM control the production of primary aerosols, we compared the POC, DOC, and CDOM concentrations of the RW, EW, and SW samples from the Geum and Seomjin coastal systems with those of the RW, EW, and SW samples from the Arctic coastal system. This was achieved by altering the color according to the total number concentrations of primary aerosol particles in the size range of 7 nm to 1 μm (Fig. 4A–C). Although the GRW and SRW samples had the highest OM concentrations, the number concentrations of primary aerosol particles were relatively low, ranging from 5.57×10^3 cm^{-3} to 1.53×10^4 cm^{-3}. It can be assumed that a small number of particles were generated under low salinity conditions, even though a large amount of OM was added to the water samples. In contrast, the GSW and SSW samples had the highest number concentrations of primary aerosol particles (1.25×10^4 cm^{-3} and 1.37×10^4 cm^{-3}), despite their relatively low OM concentrations. This implies that higher salinities were associated with higher particle concentrations, regardless of the OM content of the water samples. Hence, it seems that the dissolved inorganic salts in the water samples were more important than the OM in modulating the production of particles. In the EW samples, the number concentrations of primary aerosol particles were also higher (9.76×10^3 cm^{-3} for GEW 1 and 1.27×10^4 cm^{-3} for SEW 1) than those in the RW samples. Although

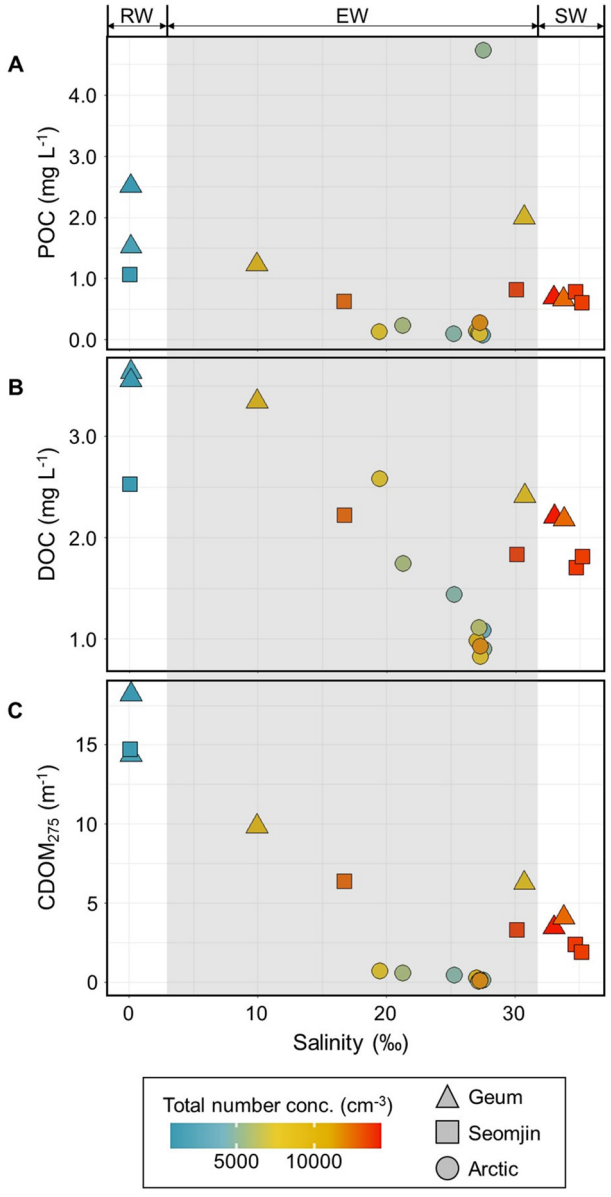

Fig. 4. Scatter plots of (A) POC, (B) DOC, and (C) CDOM versus salinity using a color scale for the total number concentration of primary aerosol particles.

the salinity of the GEW 1 and SEW 1 samples was 2–3 times lower than that of the GSW and SSW samples, the difference in the number concentrations of primary aerosol particles between the EW and SW samples was minor. Unlike the RW and SW samples, the particle number concentration trends for the GSW 1 and SSW 1 samples do not follow salinity changes, whereas higher DOM and CDOM values were observed in EW samples than in SW samples. This suggests that the characteristics of OM (predominantly of terrestrial origin) play a role in generating aerosol particles under moderate salinity conditions.

Our Geum and Seomjin results generally agreed with those of our previous study conducted in the Arctic coastal system, where terrestrial OM inputs were dominant (Park et al., 2019). In the Arctic coastal system, Park et al. (2019) found positive correlations between the number concentration of primary aerosols and sea surface OM (e.g., DOC, CDOM, Chl *a*, and TEP). This showed that primary aerosol production was affected by the salinity and OM of coastal water samples collected under moderate salinity conditions (19‰–25‰) because of the influence of discharges from the Mackenzie River. This suggests that OM of terrestrial origin enhances the concentration of primary aerosols at a given salinity level. Hence, our previous work also supports our hypothesis that terrestrial-derived OM would have a substantial effect on the production of primary aerosols under moderate salinity conditions in coastal systems.

To further examine the impact of inorganic salts on the production of primary aerosols, the number size distributions of primary aerosols produced from pure NaCl solutions for various solution concentration ranges (0.5–35‰) were determined (Fig. 5). The total number concentration of primary aerosol particles increased from 6.13×10^3 to 2.01×10^4 cm^{-3} with increasing salinity from 0.5‰ to 35‰, which was probably the result of differences in bubble coalescence (May et al., 2016). The higher ion concentrations under high salinity levels inhibit bubble coalescence, leading to the formation of smaller bubbles, thus generating higher number concentrations of primary aerosol particles. We found that the variations in the total number concentration ($(6.62 \pm 0.54) \times 10^3$ cm^{-3}) and modal diameter (55.2 ± 0 nm) of primary aerosols were minor when the NaCl concentration was <1‰, whereas both values increased proportionally from those at NaCl concentrations of 5‰ (1.21×10^4 cm^{-3}) and 10‰ (1.67×10^4 cm^{-3}). At an NaCl concentration of ≥10‰, there was little variation in the number concentration of primary aerosols (e.g., 1.78×10^4 cm^{-3} at an NaCl concentration of 35‰), indicating that the proportional increase in the number concentration of primary aerosols ceased. These results indicate that an inorganic salt concentration of at least 10‰ would be necessary to initiate the production of a high number concentration of primary aerosol particles in river–estuary–coastal ocean systems. Our results were comparable to those of the previous studies, which used different bubble generation methods (e.g., capillary tip or glass filter) to study the production of SSA particles from ocean bubble bursting (Russell and Singh, 2013; Mårtensson et al., 2003). Accordingly, sea salts appear to be an important factor for generating primary aerosols not only in the open ocean systems but also in the coastal ocean systems.

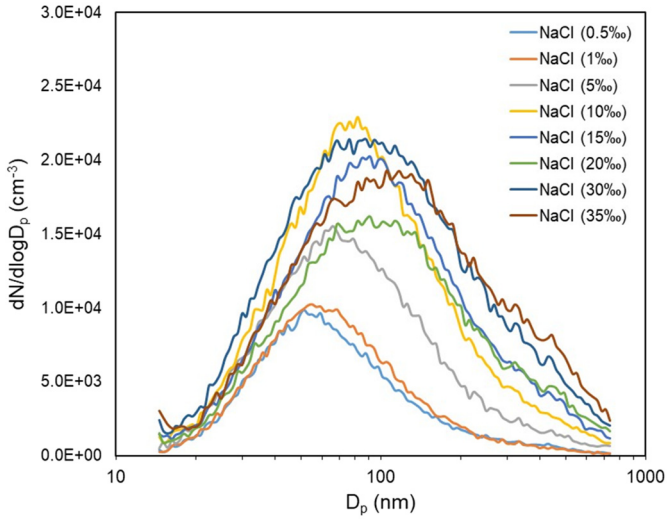

Fig. 5. The number size distribution of primary aerosol particles produced from NaCl solutions with varying salinity (0.5–35‰).

4. Conclusion and atmospheric implications

In this study, we carried out sea-spray chamber experiments using the RW, EW, and SW samples from the two temperate Korean coastal systems and the Arctic coastal system to investigate the influence of surface water properties on the number size distribution of primary aerosols. However, our study was limited with respect to the primary aerosol generation method (freshwater versus seawater) (Section S1). In the present study, the sea-spray tank system was used to generate primary aerosols for all samples for the purpose of comparison under consistent generation conditions (Section 2.2). This was because we focused on investigating the effects of the differences between inorganic salts and OM from RW and SW on primary aerosol production. In the near future, additional laboratory chamber experiments should be performed by applying different generation systems for RW and SW samples.

The mean annual global freshwater discharge from land to the ocean has been estimated to be $37{,}288 \pm 522$ km^3 yr^{-1}, which is ~7.6% of global precipitation (Dai and Trenberth, 2002). In terms of the production of primary aerosols, there are two major points to consider in such coastal oceans. First, in association with river discharge (Xu et al., 2008; Cloern et al., 2017), salinity values increase between fresh river water (low salinity of <0.5‰) to mixed water along coastlines and estuaries (moderate salinity of 0.5–29‰), and then to saline water in the oceans (high salinity of >29‰). This spatial distribution pattern of salinity is of great importance to the production of primary aerosols in river–estuary–ocean systems. Previous field campaigns in open-ocean systems demonstrated that the number concentration and diameter of SSAs depend on wind speed, sea surface temperature, and seawater particle attenuation at 660 nm, thus enabling the improvement of SSA parameterizations in global climate models (Saliba et al., 2019). Here, we suggest that the salinity associated with the inorganic salt content at the sea surface should also be incorporated into future global coupled ocean–atmospheric models to improve their accuracy in predicting the production of primary marine aerosols in river-dominated coastal systems.

Second, riverine discharges greatly affect the abundance and composition of OM in river–estuary–coastal ocean systems. Rivers transport ~0.4×10^{15} g of OM each year, of which ~60% is DOC and ~40% is POC (Raymond and Bauer, 2001). The OM in coastal oceans thus represents a substantial amount of terrestrial-derived POC and DOC (e.g., from land plants and soils), leading to a diverse reactivity of OM with ages dating back over 10^4 radiocarbon (^{14}C) years (Raymond and Bauer, 2001). Aged terrestrial-derived OM can be directly emitted from surface seawaters into the atmosphere via bubble bursting (Beaupré et al., 2019), potentially affecting oceanic and atmospheric biogeochemistry, local air quality, the coastal ocean carbon cycle, and climate. Accordingly, more work is required to better constrain the impact of terrestrial-derived OM (e.g., lignin) on the production of primary marine aerosols in coastal systems, especially for moderate salinity zones.

CRediT authorship contribution statement

Jiyeon Park: Conceptualization, Supervision, Data analysis and interpretation, Writing – original draft. **Jiyi Jang:** Visualization, Methodology. **Young Jun Yoon:** Writing – review & editing. **Sujin Kang:** Investigation. **Hyojin Kang:** Investigation. **Kihong Park:** Writing –

review & editing. **Kyung Hwa Cho:** Writing – review & editing. **Jung-Hyun Kim:** Writing – review & editing. **Manuel Dall'Osto:** Writing – review & editing. **Bang Yong Lee:** Writing – review & editing.

Declaration of competing interest

The authors declare that they have no known competing financial interests or personal relationships that could have appeared to influence the work reported in this paper.

Acknowledgements

This work was supported by grants from the Korean Government (MSIT) (NRF-2021M1A5A1065425) (KOPRI-PN21011) and from the Korean Government (MSIT) (NRF-2016R1A2B3015388) (KOPRI-PN19100). We thank Soomin Kim (KOPRI, Korea) for his assistance during the chamber experiment.

Appendix A. Supplementary data

Supplementary data to this article can be found online at https://doi.org/10.1016/j.scitotenv.2021.150866.

References

Axson, J.L., May, N.W., Colón-Bernal, I.D., Pratt, K.A., Ault, A.P., 2016. Lake spray aerosol: a chemical signature from individual ambient particles. Environ. Sci. Technol. 50 (18), 9835–9845. https://doi.org/10.1021/acs.est.6b01661.

Bates, T.S., Quinn, P.K., Frossard, A.A., Russell, L.M., Hakala, J., Petäjä, T., Kulmala, M., Covert, D.S., Cappa, C.D., Li, S.-M., Hayden, K.L., Nuaaman, I., McLaren, R., Massoli, P., Canagaratna, M.R., Onasch, T.B., Sueper, D., Worsnop, D.R., Keene, W.C., 2012. Measurements of ocean derived aerosol off the coast of California. J. Geophys. Res. Atmos. 117 (D21), D00V15. https://doi.org/10.1029/2012JD017588.

Beaupré, S.R., Kieber, D.J., Keene, W.C., Long, M.S., Maben, J.R., Lu, X., Zhu, Y., Frossard, A.A., Kinsey, J.D., Duplessis, P., Chang, R.Y.-W., Bisgrove, J., 2019. Oceanic efflux of ancient marine dissolved organic carbon in primary marine aerosol. Sci. Adv. 5 (10), eaax6535. https://doi.org/10.1126/sciadv.aax6535.

Blenkinsopp, C.E., Chaplin, J.R., 2011. Void fraction measurements and scale effects in breaking waves in freshwater and seawater. Coast. Eng. 58 (5), 417–428. https://doi.org/10.1016/j.coastaleng.2010.12.006.

Canuel, E.A., Hardison, A.K., 2016. Sources, ages, and alteration of organic matter in estuaries. Annu. Rev. Mar. Sci. 8 (1), 409–434. https://doi.org/10.1146/annurev-marine-122414-034058.

Chen, F., Zhang, L., Yang, Y., Zhang, D., 2008. Chemical and isotopic alteration of organic matter during early diagenesis: evidence from the coastal area off-shore the Pearl River estuary, South China. J. Mar. Syst. 74 (1), 372–380. https://doi.org/10.1016/j.jmarsys.2008.02.004.

Choi, J.H., Jang, E., Yoon, Y.J., Park, J.Y., Kim, T.-W., Becagli, S., Caiazzo, L., Cappelletti, D., Krejci, R., Eleftheriadis, K., Park, K.-T., Jang, K.S., 2019. Influence of biogenic organics on the chemical composition of Arctic aerosols. Glob. Biogeochem. Cycles 33 (10), 1238–1250. https://doi.org/10.1029/2019GB006226.

Cloern, J.E., Jassby, A.D., Schraga, T., Kress, E.S., Martin, C.A., 2017. Ecosystem variability along the estuarine salinity gradient: examples from long-term study of San Francisco Bay. Limnol. Oceanogr. 62 (S1), S272–S291. https://doi.org/10.1002/lno.10537.

Coble, P.G., 2007. Marine optical biogeochemistry: the chemistry of ocean color. Chem. Rev. 107 (2), 402–418. https://doi.org/10.1021/cr050350+.

Cochran, R.E., Ryder, O.S., Grassian, V.H., Prather, K.A., 2017. Sea spray aerosol: the chemical link between the oceans, atmosphere, and climate. Acc. Chem. Res. 50 (3), 599–604. https://doi.org/10.1021/acs.accounts.6b00603.

Dai, A., Trenberth, K.E., 2002. Estimates of freshwater discharge from continents latitudinal and seasonal variations. J. Hydrometeorol. 3 (6), 660–687. https://doi.org/10.1175/1525-7541(2002)003%3C0660:EOFDFC%3E2.0.CO;2.

Facchini, M.C., Rinaldi, M., Decesari, S., Carbone, C., Finessi, E., Mircea, M., Fuzzi, S., Ceburnis, D., Flanagan, R., Nilsson, E.D., de Leeuw, G., Martino, M., Woeltjen, J., O'Dowd, C.D., 2008. Primary submicron marine aerosol dominated by insoluble organic colloids and aggregates. Geophys. Res. Lett. 35 (17), L17814. https://doi.org/10.1029/2008GL034210.

Galy, V., France-Lanord, C., Beyssac, O., Faure, P., Kudrass, H., Palhol, F., 2007. Efficient organic carbon burial in the Bengal fan sustained by the Himalayan erosional system. Nature 450 (7168), 407–410. https://doi.org/10.1038/nature06273.

Gantt, B., Meskhidze, N., Kamykowski, D., 2009. A new physically-based quantification of marine isoprene and primary organic aerosol emissions. Atmos. Chem. Phys. 9, 4915–4927. https://doi.org/10.5194/acp-9-4915-2009.

Gardner, W.D., Mishonov, A.V., Richardson, M.J., 2006. Global POC concentration from in-situ and satellite data. Deep-Sea Res. II 53 (5–7), 718–740. https://doi.org/10.1016/j.dsr2.2006.01.029.

Gong, S.L., 2003. A parameterization of sea-salt aerosol source function for sub- and super-micron particles. Glob. Biogeochem. Cycles 17 (4), 1097. https://doi.org/10.1029/2003GB002079.

Goni, M.A., Monacci, N., Gisewhite, R., Crockett, J., Nittrouer, C., Ogston, A., Alin, S.R., Aalto, R., 2008. Terrigenous organic matter in sediments from the Fly River delta-clinoform system (Papua New Guinea). J. Geophys. Res. Earth Surf. 113 (F1), F01S10. https://doi.org/10.1029/2006JF000653.

Guo, W., Ye, F., Xu, S., Jia, G., 2015. Seasonal variation in sources and processing of particulate organic carbon in the Pearl River estuary, South China. 167, 540–548. https://doi.org/10.1016/j.ecss.2015.11.004.

Hao, C., Lissemore, L., Nguyen, B., Kleywegt, S., Yang, P., Solomon, K., 2006. Determination of pharmaceuticals in environmental waters by liquid chromatography/electrospray ionization/tandem mass spectrometry. Anal. Bioanal. Chem. 384 (2), 505–513. https://doi.org/10.1007/s00216-005-0199-y.

Huot, Y., Babin, M., Bruyant, F., Grob, C., Twardowski, M., Claustre, H., 2007. Does chlorophyll a provide the best index of phytoplankton biomass for primary productivity studies? Biogeosci. Discuss. 4 (2), 707–745. https://hal.archives-ouvertes.fr/hal-00330232.

Kang, S., Kim, J.-H., Kim, D., Song, H., Ryu, J.-S., Ock, G., Shin, K.-H., 2019. Temporal variation in riverine organic carbon concentrations and fluxes in two contrasting estuary systems: Geum and Seomjin, South Korea. 133, 105126. https://doi.org/10.1016/j.envint.2019.105126.

Kang, S., Kim, J.-H., Hwang, J.H., Bong, Y.S., Ryu, J.-S., Shin, K.-H., 2020. Seasonal contrast of particulate organic carbon (POC) characteristics in the Geum and Seomjin estuary systems (South Korea) revealed by carbon isotope (δ13C and Δ14C) analyses. Water Res. 187, 116442. https://doi.org/10.1016/j.watres.2020.116442.

Li, J., Yu, Q., Tian, Y.Q., Becker, B.L., 2017. Remote sensing estimation of colored dissolved organic matter (CDOM) in optically shallow waters. P&RS 128, 98–110. https://doi.org/10.1016/j.isprsjprs.2017.03.015.

Mannino, A., Russ, M.E., Hooker, S.B., 2008. Algorithm development and validation for satellite-derived distributions of DOC and CDOM in the U.S. Middle Atlantic Bight. J. Geophys. Res. Oceans 113 (C7), C07051. https://doi.org/10.1029/2007JC004493.

Mårtensson, E.M., Nilsson, E.D., de Leeuw, G., Cohen, L.H., Hansson, H.-C., 2003. Laboratory simulations and parameterization of the primary marine aerosol production. J. Geophys. Res. Atmos. 108 (D9), 4297. https://doi.org/10.1029/2002JD002263.

Martin, P., Cherukuru, N., Tan, A.S.Y., Sanwlani, N., Mujahid, A., Müller, M., 2018. Distribution and cycling of terrigenous dissolved organic carbon in peatland-draining rivers and coastal waters of Sarawak, Borneo. 15 (22), 6847–6865. https://doi.org/10.5194/bg-15-6847-2018.

Marwick, T.R., Tamooh, F., Teodoru, C.R., Borges, A.V., Darchambeau, F., Bouillon, S., 2015. The age of river-transported carbon: a global perspective. Glob. Biogeochem. Cycles 29 (2), 122–137. https://doi.org/10.1002/2014GB004911.

May, N.W., Axson, J.L., Watson, A., Pratt, K.A., Ault, A.P., 2016. Lake spray aerosol generation: a method for producing representative particles from freshwater wave breaking. Atmos. Meas. Tech. 9 (9), 4311–4325. https://doi.org/10.5194/amt-9-4311-2016.

Meyers, P.A., 1997. Organic geochemical proxies of paleoceanographic, paleolimnologic, and paleoclimatic processes. Org. Geochem. 27 (5), 213–250. https://doi.org/10.1016/S0146-6380(97)00049-1.

Nebbioso, A., Piccolo, A., 2013. Molecular characterization of dissolved organic matter (DOM): a critical review. Anal. Bioanal. Chem. 405 (1), 109–124. https://doi.org/10.1007/s00216-012-6363-2.

O'Dowd, C.D., Facchini, M.C., Cavalli, F., Ceburnis, D., Mircea, M., Decesari, S., Fuzzi, S., Yoon, Y.J., Putaud, J.P., 2004. Biogenically driven organic contribution to marine aerosol. Nature 431 (7009), 676–680. https://doi.org/10.1038/nature02959.

O'Dowd, C.D., Langmann, B., Varghese, S., Scannell, C., Ceburnis, D., Facchini, M.C., 2008. A combined organic-inorganic sea-spray source function. Geophys. Res. Lett. 35 (1), L01801. https://doi.org/10.1029/2007GL030331.

Park, J., Dall'Osto, M., Park, K., Kim, J.-H., Park, J., Park, K.-T., Hwang, C.Y., Jang, G.I., Gim, Y., Kang, S., Park, S., Jin, Y.K., Yum, S.S., Simó, R., Yoon, Y.J., 2019. Arctic primary aerosol production strongly influenced by riverine organic matter. Environ. Sci. Technol. 53 (15), 8621–8630. https://doi.org/10.1021/acs.est.9b03399.

Partanen, A.I., Dunne, E.M., Bergman, T., Laakso, A., Kokkola, H., Ovadnevaite, J., Sogacheva, L., Baisnée, D., Sciare, J., Manders, A., O'Dowd, C., de Leeuw, G., Korhonen, H., 2014. Global modelling of direct and indirect effects of sea spray aerosol using a source function encapsulating wave state. Atmos. Chem. Phys. 14 (21), 11731–11752. https://doi.org/10.5194/acp-14-11731-2014.

Peterson, B.J., Fry, B., 1987. Stable isotopes in ecosystem studies. Annu. Rev. Ecol. Evol. Syst. 18, 293–320.

Prather, K.A., Bertram, T.H., Grassian, V.H., Deane, G.B., Stokes, M.D., DeMott, P.J., Aluwihare, L.I., Palenik, B.P., Azam, F., Seinfeld, J.H., Moffet, R.C., Molina, M.J., Cappa, C.D., Geiger, F.M., Roberts, G.C., Russell, L.M., Ault, A.P., Baltrusaitis, J., Collins, D.B., Corrigan, C.E., Cuadra-Rodriguez, L.A., Ebben, C.J., Forestieri, S.D., Guasco, T.L., Hersey, S.P., Kim, M.J., Lambert, W.F., Modini, R.L., Mui, W., Pedler, B.E., Ruppel, M.J., Ryder, O.S., Schoepp, N.G., Sullivan, R.C., Zhao, D., 2013. Bringing the ocean into the laboratory to probe the chemical complexity of sea spray aerosol. Proc. Natl. Acad. Sci. U. S. A. 110 (19), 7550–7555. https://doi.org/10.1073/pnas.1300262110.

Quinn, P.K., Bates, T.S., Schulz, K.S., Coffman, D.J., Frossard, A.A., Russell, L.M., Keene, W.C., Kieber, D.J., 2014. Contribution of sea surface carbon pool to organic matter enrichment in sea spray aerosol. Nat. Geosci. 7 (3), 228–232. https://doi.org/10.1038/ngeo2092.

Quinn, P.K., Collins, D.B., Grassian, V.H., Prather, K.A., Bates, T.S., 2015. Chemistry and related properties of freshly emitted sea spray aerosol. Chem. Rev. 115 (10), 4383–4399. https://doi.org/10.1021/cr500713g.

Raymond, P.A., Bauer, J.E., 2001. Use of 14C and 13C natural abundances for evaluating riverine, estuarine, and coastal DOC and POC sources and cycling: a review and

synthesis. Org. Geochem. 32 (4), 469–485. https://doi.org/10.1016/S0146-6380(00)00190-X.
Russell, L.M., Singh, E.G., 2013. Submicron salt particle production in bubble bursting. Aerosol Sci. Technol. 40 (9), 664–671. https://doi.org/10.1080/02786820600793951.
Saliba, G., Chen, C.-L., Lewis, S., Russell, L., Rivellini, L.-H., Lee, A., Quinn, P., Bates, T., Haëntjens, N., Boss, E., Karp-Boss, L., Baetge, N., Carlson, C., Behrenfeld, M., 2019. Factors driving the seasonal and hourly variability of sea-spray aerosol number in the North Atlantic. Proc. Natl. Acad. Sci. U. S. A. 116 (41), 20309–20314. https://doi.org/10.1073/pnas.1907574116.
Schwier, A.N., Rose, C., Asmi, E., Ebling, A.M., Landing, W.M., Marro, S., Pedrotti, M.L., Sallon, A., Iuculano, F., Agusti, S., Tsiola, A., Pitta, P., Louis, J., Guieu, C., Gazeau, F., Sellegri, K., 2015. Primary marine aerosol emissions from the Mediterranean Sea during pre-bloom and oligotrophic conditions: correlations to seawater chlorophyll a from a mesocosm study. Atmos. Chem. Phys. 15 (14), 7961–7976. https://doi.org/10.5194/acp-15-7961-2015.
Sciare, J., Favez, O., Sarda-Estève, R., Oikonomou, K., Cachier, H., Kazan, V., 2009. Long-term observations of carbonaceous aerosols in the Austral Ocean atmosphere: evidence of a biogenic marine organic source. J. Geophys. Res. Atmos. 114 (D15), D15302. https://doi.org/10.1029/2009JD011998.
Sellegri, K., O'Dowd, C.D., Yoon, Y.J., Jennings, S.G., de Leeuw, G., 2006. Surfactants and submicron sea spray generation. J. Geophys. Res. Atmos. 111 (D22), D22215. https://doi.org/10.1029/2005JD006658.
Seo, J.-H., Kang, I., Yang, S.-J., Cho, J.-C., 2017. Characterization of spatial distribution of the bacterial community in the South Sea of Korea. PLoS One 12 (3), e0174159. https://doi.org/10.1371/journal.pone.0174159.
Slade, J.H., VanReken, T.M., Mwaniki, G.R., Bertman, S., Stirm, B., Shepson, P.B., 2010. Aerosol production from the surface of the Great Lakes. Geophys. Res. Lett. 37 (18), L18807. https://doi.org/10.1029/2010GL043852.
Small, L.F., McIntire, C.D., MacDonald, K.B., Lara-Lara, J.R., Frey, B.E., Amspoker, M.C., Winfield, T., 1990. Primary production, plant and detrital biomass, and particle transport in the Columbia River Estuary. Prog. Oceanogr. 25 (1), 175–210. https://doi.org/10.1016/0079-6611(90)90007-O.
Spracklen, D.V., Arnold, S.R., Sciare, J., Carslaw, K.S., Pio, C., 2008. Globally significant oceanic source of organic carbon aerosol. Geophys. Res. Lett. 35 (12), L12811. https://doi.org/10.1029/2008GL033359.
Vignati, E., Facchini, M.C., Rinaldi, M., Scannell, C., Ceburnis, D., Sciare, J., Kanakidou, M., Myriokefalitakis, S., Dentener, F., O'Dowd, C.D., 2010. Global scale emission and distribution of sea-spray aerosol: sea-salt and organic enrichment. Atmos. Environ. 44 (5), 670–677. https://doi.org/10.1016/j.atmosenv.2009.11.013.
Wang, X., Deane, G.B., Moore, K.A., Ryder, O.S., Stokes, M.D., Beall, C.M., Collins, D.B., Santander, M.V., Burrows, S.M., Sultana, C.M., Prather, K.A., 2017. The role of jet and film drops in controlling the mixing state of submicron sea spray aerosol particles. Proc. Natl. Acad. Sci. U. S. A. 114 (27), 6978–6983. https://doi.org/10.1073/pnas.1702420114.
Ward, N.D., Megonigal, J.P., Bond-Lamberty, B., Bailey, V.L., Butman, D., Canuel, E.A., Diefenderfer, H., Ganju, N.K., Goñi, M.A., Graham, E.B., Hopkinson, C.S., Khangaonkar, T., Langley, J.A., McDowell, N.G., Myers-Pigg, A.N., Neumann, R.B., Osburn, C.L., Price, R.M., Rowland, J., Sengupta, A., Simard, M., Thornton, P.E., Tzortziou, M., Vargas, R., Weisenhorn, P.B., Windham-Myers, L., 2020. Representing the function and sensitivity of coastal interfaces in earth system models. Nat. Commun. 11 (1), 2458. https://doi.org/10.1038/s41467-020-16236-2.
Wei, H., Shi, J., Lu, Y., Peng, Y., 2010. Interannual and long-term hydrographic changes in the Yellow Sea during 1977–1998. Deep-Sea Res. PT. II 57 (11), 1025–1034. https://doi.org/10.1016/j.dsr2.2010.02.004.
Whittle, K.J., 1977. Marine organisms and their contribution to organic matter in the ocean. Mar. Chem. 5 (4), 381–411. https://doi.org/10.1016/0304-4203(77)90030-5.
Williams, W.D., Sherwood, J.E., 1994. Definition and measurement of salinity in salt lakes. Int. J. Salt Lake Res. 3 (1), 53–63. https://doi.org/10.1007/BF01990642.
Xu, H., Lin, J., Wang, D., 2008. Numerical study on salinity stratification in the Pamlico River Estuary. Estuar. Coast. Shelf Sci. 80 (1), 74–84. https://doi.org/10.1016/j.ecss.2008.07.014.
Ye, F., Guo, W., Shi, Z., Jia, G., Wei, G., 2017. Seasonal dynamics of particulate organic matter and its response to flooding in the Pearl River Estuary, China, revealed by stable isotope (δ13C and δ15N) analyses. J. Geophys. Res. Oceans 122 (8), 6835–6856. https://doi.org/10.1002/2017JC012931.
Yoon Il, B., Woo, S.-B., 2013. Correlation between freshwater discharge and salinity intrusion in the Han River Estuary, South Korea. 65 (10065), 1247–1252. https://doi.org/10.2112/SI65-211.1.